Eur. Phys. J. D **44**, 93–107 (2007)
DOI: 10.1140/epjd/e2007-00152-3

THE EUROPEAN PHYSICAL JOURNAL D

Structure and dynamics of cationic van-der-Waals clusters

III. Binding and structure of Ar_nHCl^+ clusters

T. Ritschel[1], P.J. Kuntz[2], and L. Zülicke[1,a]

[1] Universität Potsdam, Institut für Chemie, Karl-Liebknecht-Straße 24-25, 14476 Golm, Germany
[2] Hahn-Meitner-Institut, Abteilung SF5, Glienicker Straße 100, 14109 Berlin, Germany

Received 18 January 2007 / Received in final form 22 March 2007
Published online 11 May 2007 –

Abstract. Ar_nHCl^+ van-der-Waals clusters for $n = 1$–13 are investigated with the "minimal diatomics-in-molecules (DIM) model" using ab-initio input data obtained from multi-reference configuration-interaction calculations plus subsequent projection onto valence-bond wavefunctions. The results for the complexes with $n = 1$–3 are checked against ab-initio calculations at the coupled-cluster (CCSD) level with the same one-electron atomic basis set as for the input data generation (aug-cc-pVTZ from Dunning). In addition to the electronic ground state, the first excited $^2A'$ state for the triatomic complex ($n = 1$) is also studied. The results from the DIM model are shown to be in fair agreement with those from advanced conventional ab-initio calculations, although there are differences in detail. The comparison justifies the extension of the DIM approach to $n > 3$. Systematic analysis of the local minima of the multi-dimensional potential-energy surfaces (PESs), carried out with the combined method described in part I (Monte-Carlo sampling plus subsequent steepest-descent optimization), reveals simple building-up regularities for the most stable structures (i.e. those corresponding to the global PES minimum) at each n: apart from always having a nearly linear $(Ar–H–Cl)^+$ fragment as core, the aggregates show little or no symmetry. Secondary local minima are also determined and their structures interpreted. The PESs for the low-lying excited states reveal a much more complicated topography compared to the Ar_nH^+ clusters allowing a variety of photo-processes. The energy level sequence of the first five excited electronic states and the stability of the clusters in these states is studied as a function of the cluster size n.

PACS. 31.15.Ar Ab initio calculations – 31.50.Bc Potential energy surfaces for ground electronic states – 31.50.Df Potential energy surfaces for excited electronic states – 36.40.-c Atomic and molecular clusters – 36.40.Wa Charged clusters – 36.40.Qv Stability and fragmentation of clusters

1 Introduction

With papers I and II of this series [1,2] we started an extensive investigation of the structural and dynamical properties of positively charged inhomogeneous clusters of the type Rg_nM^+, where Rg denotes a rare-gas atom and M some atom or small molecule. The motivation for undertaking this task as well as an overview of earlier studies together with the relevant references are given therein.

The special features distinguishing our study from earlier research are (i) the systematic extension to medium-sized clusters (up to $n = 35$ in parts I and II for Ar_nH^+, the rare-gas clusters with the simplest conceivable ionic impurity M^+, namely the proton H^+), (ii) the investigation of excited electronic states, and (iii) the treatment of intra-cluster dynamics as well as collision processes. The theoretical method for doing this must clearly be very efficient in order to master the problems connected with the increasing number of nuclear degrees of freedom, and it must be capable of generating potential-energy surfaces (PESs) for (low-lying) excited electronic states with the same facility as for the ground state. These demands are satisfied by what we call our "minimal ab-initio diatomics-in-molecules (DIM) model" as described in part I [1].

The promising results for the medium-sized protonated argon clusters, Ar_nH^+ [1,2], encouraged us to tackle the more complicated case with the impurity $M^+ = HCl^+$. In contrast to the "naked" proton, the HCl^+ molecular ion has an electronic structure, so we therefore expect a much more difficult electronic structure problem in the aggregates Ar_nHCl^+. Indeed, as earlier studies on the simplest triatomic member of this class of systems, $ArHCl^+$, have shown [3–5], we are faced with a number of energetically nearly degenerate electronic states with complicated crossing and pseudo-crossing behaviour. This constitutes a hard test case for our simple DIM model, and it will be interesting to see, whether and to what extent the problems can be overcome.

[a] e-mail: zuelicke@tc1.chem.uni-potsdam.de

The organization of the present paper is as follows: Section 2 sketches the methodology (described in detail in part I) and Section 3 presents the necessary DIM input information for the relevant diatomic fragments. The results of the calculations on the Ar_nHCl^+ aggregates are reported and discussed in Section 4, first for the triatomic complex $ArHCl^+$ and then for the larger clusters; some findings for the excited electronic states are included here as well. Section 5 gives the summary and conclusions.

2 Methodology

As in the study on the protonated argon clusters [1,2], the PES calculations performed here rest on the usual adiabatic (Born-Oppenheimer) separation of electronic and nuclear degrees of freedom, giving the potential-energy function for the nuclear motion as the sum of the total electrostatic nuclear repulsion energy plus the total energy of the electron cloud of the whole system. The latter must be determined from an approximate solution to the electronic Schrödinger equation for each nuclear geometry needed. Once again, we neglect relativistic effects in the present case as well — they should be of minor importance compared with the errors arising from the DIM approach itself.

The overall strategy and level of sophistication — the "minimal ab-initio DIM model" — is exactly the same as in part I [1], to which we refer the reader for more details:

- The quantum-mechanical method for determining the potential-energy surfaces of the Ar_nHCl^+ aggregates is the *minimal* DIM model. This is defined by including all atomic and diatomic fragment electronic states that lead to doublet states of the whole cluster and that lie energetically not more than 10 eV above the respective fragment ground states. For Ar_nHCl^+ the *minimal* DIM basis set includes the following atomic states:

  $Ar(^1S)$, $Ar^+(^2P^\circ)$, $Cl(^2P^\circ)$, $Cl^+(^3P, ^1D, ^1S)$, $Cl^-(^1S)$, $H(^2S)$.

  The diatomic states implied by this basis are

  $ArH(X^2\Sigma^+)$, $ArH^+(X^1\Sigma^+, 1^1\Pi, 2^1\Sigma^+, 1^3\Pi, 1^3\Sigma^+)$, $ArH^{++}(X^2\Pi, 1^2\Sigma^+)$,
  $Ar_2(X^1\Sigma_g^+)$, $Ar_2^+(X^2\Sigma_u^+, 1^2\Pi_g, 1^2\Pi_u, 1^2\Sigma_g^+)$,
  $HCl(X^1\Sigma^+, 1^3\Pi, 1^1\Pi, 1^3\Sigma^+, 2^1\Sigma^+)$,
  $HCl^+(X^2\Pi, 2^2\Pi, 3^2\Pi, 1^2\Sigma^+, 2^2\Sigma^+, 3^2\Sigma^+, 1^2\Sigma^-, 1^2\Delta)$,
  $ArCl(X^2\Sigma^+, 1^2\Pi, 2^2\Sigma^+, 2^2\Pi)$,
  $ArCl^+(X^1\Sigma^+, 1^1\Pi, 1^1\Delta, 2^1\Sigma^+, 2^1\Pi, 1^1\Sigma^-, 2^1\Delta, 3^1\Sigma^+, 3^1\Pi, 4^1\Sigma^+, 1^3\Pi, 1^3\Sigma^-, 2^3\Pi, 1^3\Sigma^+, 1^3\Delta, 3^3\Pi, 2^3\Sigma^-, 2^3\Sigma^+)$,
  $ArCl^-$ $(X^1\Sigma^+)$.

  Altogether there are 8 atomic and 49 diatomic fragment states (in contrast to the 3 atomic and 9 diatomic fragment states needed for Ar_nH^+). The number of resulting DIM (polyatomic) basis functions (i.e. the dimension of the DIM matrix to be diagonalized) is $21n + 12$ (again much larger than for Ar_nH^+, where it was only $3n + 1$).
- The fragment input data for the DIM procedure, namely the atomic state energies and the diatomic fragment Hamiltonian matrix elements for the different electronic fragment states as functions of the internuclear distance, are accurately calculated using an internally contracted multi-reference configuration-interaction with single and double excitations (ic-MRCI) procedure including a generalized Davidson correction for estimating the energetic contributions of higher-order excitations (icMRCI+Q). For this part of the task we employed the MOLPRO suite of programs [6] and for the one-electron atomic-orbital (AO) basis set we chose the aug-cc-pVTZ set of Woon and Dunning [7] (which includes several diffuse functions for each atom) contracted to a total of $50n+73$ atomic basis functions.
- The projection procedure of Kuntz and Schreiber [8] was used in order to convert the diatomic fragment matrix elements as functions of the internuclear distance from the molecular orbital (MO) based CI form to the valence-bond (VB) form needed in the DIM ansatz. This projection provides the mixing coefficients arising in the linear combinations of VB configurations belonging to the same symmetry. Such mixing appears in 12 diatomic fragments in the present system, requiring altogether 25 coefficients (in contrast to Ar_nH^+ with only one mixing coefficient).
- For cross-checking calculations at selected nuclear geometries (i.e. single PES points), a coupled cluster approach with single and double excitations (CCSD), also available in the MOLPRO package of ab-initio programs [6], was utilized, again with the same AO basis set.
- The search for the relevant stationary points on the multi-dimensional PESs for the adiabatic electronic states of the clusters was accomplished by means of the same method used for Ar_nH^+ in part I: a Monte-Carlo generation of initial geometries combined with a subsequent steepest-descent optimization procedure.

It should be pointed out that the one-electron AO basis set mentioned above is common to all the calculations carried out in this study.

3 Diatomic fragment data for the DIM input

First of all, we give an overview of the main diatomic fragment data employed in the subsequent DIM treatment. More details, including the results for the atomic state calculations, can be found in [9] and/or obtained on request from one of the present authors[1].

The potential-energy curves (PECs) for the neutral and ionic diatomic fragments are shown in Figures 1a–1h. Those already presented in part I [1] for the Ar_2^+ and Ar_2 dimers are omitted but, for the ArH^+ fragment, all states are shown in order to have a more complete picture of the low-energy term structure.

[1] e-mail: ritschel@chem.uni-potsdam.de

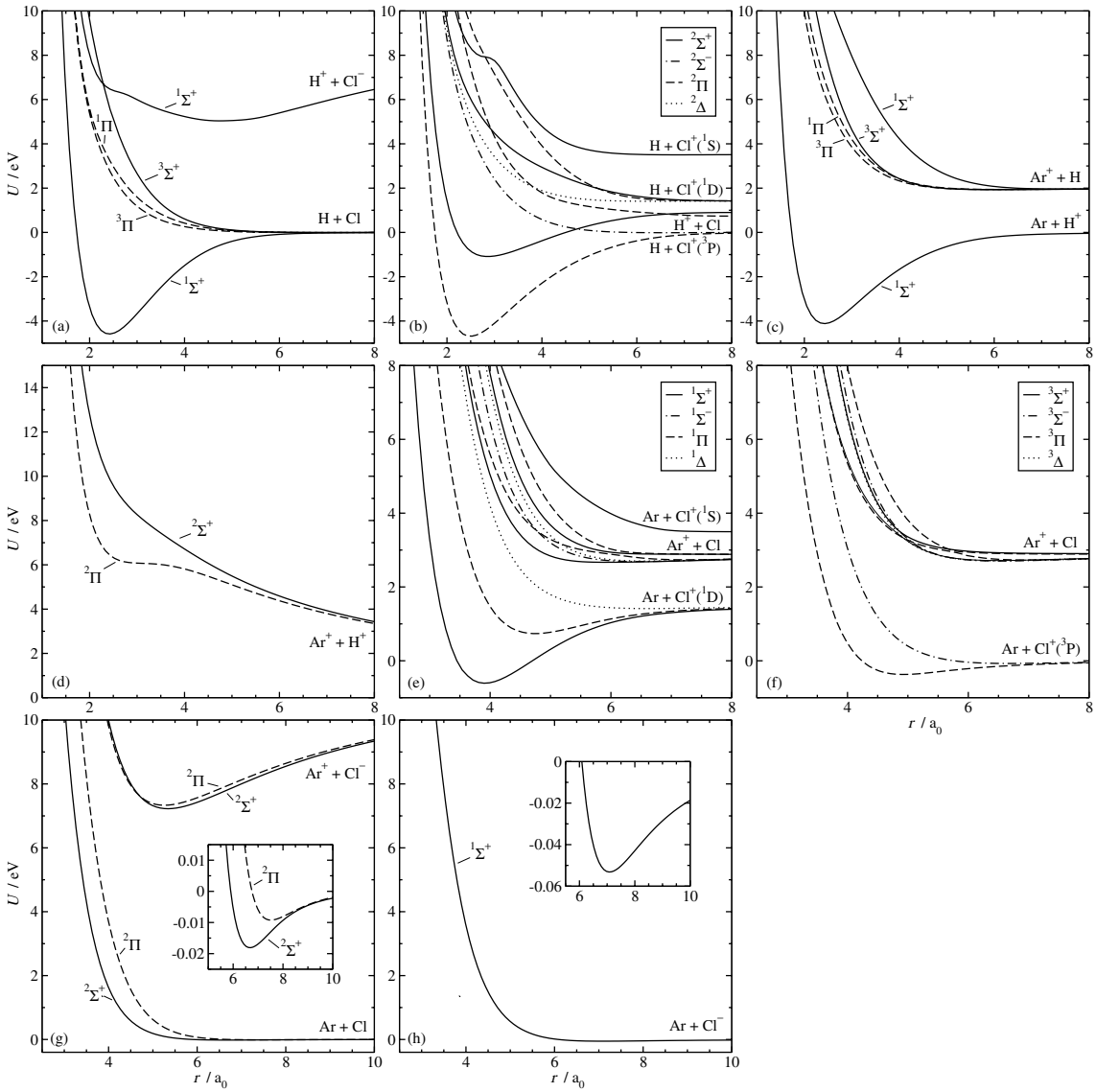

Fig. 1. Potential-energy curves for relevant diatomic fragment states in the "minimal ab-initio DIM model" for Ar_nHCl^+. (a) HCl, (b) HCl^+, (c) ArH^+, (d) ArH^{++}, (e) $ArCl^+$ (singlet states), (f) $ArCl^+$ (triplet states), (g) ArCl, (h) $ArCl^-$.

To give an impression of the accuracy of our calculations, molecular characteristics for the electronic ground states of some of the diatomic fragments are compiled in Table 1 and compared with experiment where possible. Some of the species have still not been detected and experimental information about the excited electronic states is even scarcer. For van-der-Waals molecules (flat PECs), the values of r_e and D_e have, of course, lower reliability: r_e has an uncertainty of about 0.1 a_0 in contrast to about 0.01 a_0 for valence bonds; the deviation of D_e is several meV, which is, after all, a considerable part of the absolute value for the weak bonds. For the strong bonds, the deviation is about 0.1 eV, which is, however, a much smaller relative error. Using the counterpoise method [12], the basis-set superposition error (BSSE) was estimated to lead to errors in the bond lengths of magnitude 0.01 a_0 or less for the strong bonds and 0.1 a_0 for the weak bonds; for the dissociation energy, the corresponding error estimates

Table 1. Molecular characteristics of diatomic fragments of Ar_nHCl^+ clusters in their electronic ground states as obtained from MRCI calculations (in parentheses: experimental data).

Fragment (State)	r_e^a a_0	D_e^a eV	ω cm^{-1}	Exp. Reference
HCl ($X^1\Sigma^+$)	2.42	4.59	2920.4	
	(2.41)	(4.62)	(2990.9)	[10]
HCl^+ ($X^2\Pi$)	2.49	4.69	2620.2	
	(2.48)	(4.82)	(2673.7)	[10]
ArCl ($X^2\Sigma^+$)	6.68	0.018	39.1	
	(7.05)	(0.017)	(35.6)	[11]
$ArCl^+$ ($X^1\Sigma^+$)	3.91	2.11	437.2	
	(–)	(–)	(–)	
$ArCl^-$ ($X^1\Sigma^+$)	7.09	0.053	49.4	
	(7.01)	(0.065)	(58.5)	[11]

[a] r_e is the internuclear distance at which the potential-energy curve has its minimum; D_e is the depth of the minimum relative to the dissociation limit.

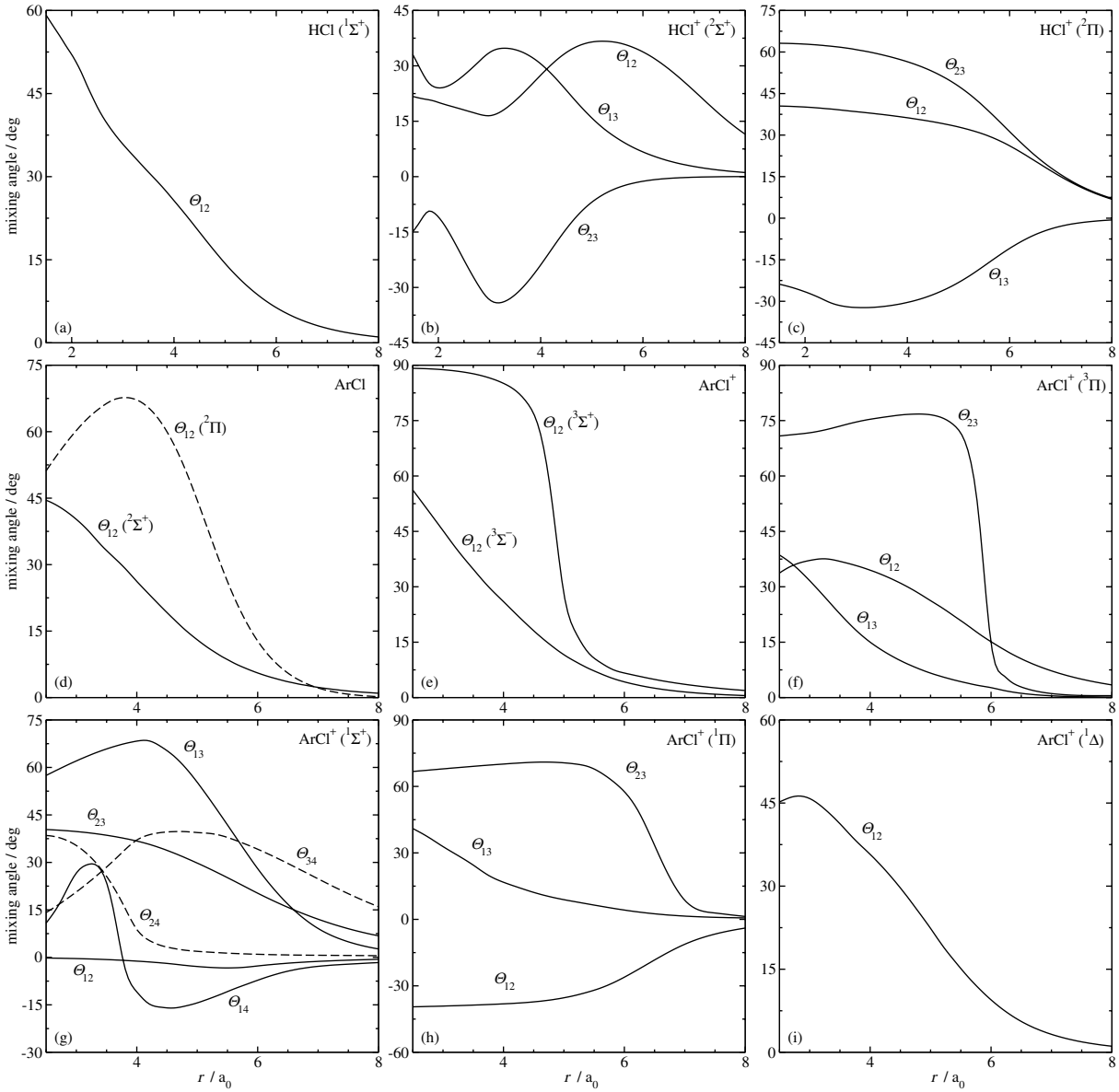

Fig. 2. VB configuration "mixing angles" Θ_{ij} of states i and j of the same symmetry as a function of the internuclear distance r. For clarity, some of the curves are dashed. (a) HCl ($^1\Sigma^+$), (b) HCl$^+$ ($^2\Sigma^+$), (c) HCl$^+$ ($^2\Pi$), (d) ArCl ($^2\Sigma^+$ and $^2\Pi$), (e) ArCl$^+$ ($^3\Sigma^+$ and $^3\Sigma^-$), (f) ArCl$^+$ ($^3\Pi$), (g) ArCl$^+$ ($^1\Sigma^+$), (h) ArCl$^+$ ($^1\Pi$), (i) ArCl$^+$ ($^1\Delta$).

are 0.01 eV and a few meV respectively. Altogether, the precision of the diatomic fragment data is of a rather high level, as expected, and should suffice for present purposes.

From the list of fragment states in Section 2, it is seen that, in addition to the two $^1\Sigma^+$ states of the fragment ArH^+ already appearing in the minimal DIM treatment of the Ar_nH^+ clusters, there are 11 diatomic fragment manifolds containing more than one state. A list of these manifolds, together with their symmetries and number of states, follows:

- two $^1\Sigma^+$ states of HCl;
- three $^2\Sigma^+$ states and three $^2\Pi$ states of HCl^+;
- two $^2\Sigma^+$ states and two $^2\Pi$ states of ArCl;
- four $^1\Sigma^+$, three $^1\Pi$, two $^1\Delta$, two $^3\Sigma^+$, two $^3\Sigma^-$, and three $^3\Pi$ states of $ArCl^+$.

All these mixings must be taken into account, and the coefficients of the corresponding AO configurations in the VB ansatz for the diatomic fragment wavefunctions must be determined by the projection procedure mentioned above. In the simple example of HCl, the normalized coefficients c_1 and c_2 of the ground and the lowest excited $^1\Sigma^+$ configurations are written as $\cos\Theta_{12}$ and $\sin\Theta_{12}$, respectively, where Θ_{12} is called the "mixing angle". For more complicated cases with mixing of three or four VB configurations, this procedure can be generalized (as explained, e.g., in [13]). The results are seen in Figures 2a–2i (except for the mixing in ArH^+; for this see Fig. 2 in part I [1]) as functions of the internuclear distance. These graphs reflect the variation in the dominating bonding character over the relevant distance regions, but this topic — the

binding properties of the diatomics — will not be discussed here in detail.

The diatomic fragment potential-energy functions as well as the mixing functions are used to compute Hamiltonian matrices for the diatomic fragments. The elements of these matrices are carefully fitted to appropriate analytic (or spline) functions and in this form are used for DIM input. Again, the details will not be given here[2].

4 Results and discussion

Owing to the large number of fragment states and VB mixings, even the simplest DIM model for Ar_nHCl^+ clusters is much more difficult to handle than those for Ar_n^+ and Ar_nH^+. In fact, even the smallest complex, $ArHCl^+$, is not easy to describe accurately, and this holds not only for DIM but also for the advanced conventional quantum-mechanical approaches (mentioned in Sect. 2) required for generating the fragment data (see Sect. 3) as well as cross-checking the results from DIM for the small Ar_nHCl^+ complexes (vide infra). In the light of this remark one should be aware that the accuracy (i.e. the number of digits) of the theoretical results is meaningful only for comparisons within the theoretical context. If detailed predictions or comparison with experiment is desired, a special estimation of the errors must be made.

4.1 The $ArHCl^+$ complex

To define the geometrical arrangement of the three nuclei in $ArHCl^+$ we use the H–Cl and Ar–Cl internuclear distances r_1 and r_2 respectively and the enclosed angle $\alpha = \angle$ArClH, as the set of body-fixed internal coordinates.

4.1.1 Electronic ground state of $ArHCl^+$

As mentioned in the introduction, there are several recent theoretical investigations of the triatomic complex $ArHCl^+$ [3–5], so that we have at our disposal a large amount of information for judging the reliability and quality of the present DIM results.

The topography of the DIM ground-state PES is illustrated in Figures 3 and 4. The former shows a contour-line diagram of the potential as a function of the position of the proton in a plane containing the Ar and Cl nuclei fixed at a distance of 6.2 a_0. Figure 4 presents a contour-line plot of the potential-energy function $U(r_2, \alpha)$ for the same PES with the H–Cl distance fixed at $r_1 = 2.5\ a_0$. This H–Cl distance remains approximately constant for all low-energy nuclear configurations in the electronic ground state. The molecular characteristics at the stationary points on the ground-state PES determined from recent theoretical studies on $ArHCl^+$ are collected in Table 2. Above all we note that the new ab-initio CCSD and MRCI calculations performed in the present study agree well with the earlier investigations [5]. What can be seen from these results is the following:

1. All of the recent studies agree that the triatomic complex $ArHCl^+$ in its electronic ground state is stable in two geometrical forms: one exactly linear, $(Ar–H–Cl)^+$, with the proton between the two heavy nuclei, and one nearly rectangular with the proton twisted out of the Ar–Cl axis, the angle $\angle$ArClH being not much different from 90°.
   The remark about stability also holds when the zero-point energy (ZPE) contributions are included, as can

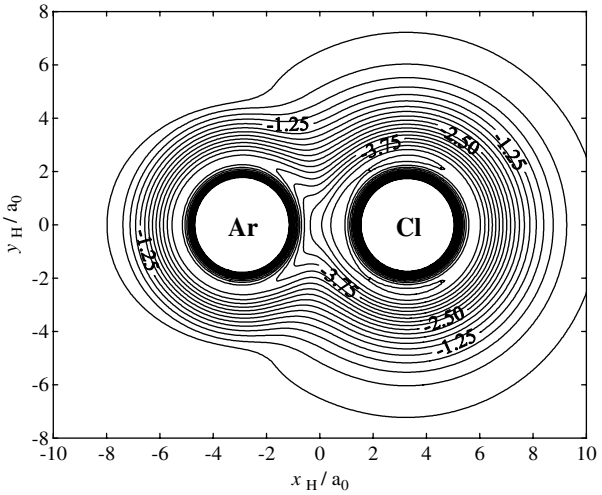

Fig. 3. DIM potential energy contour-line diagram for the proton in a plane containing the Ar and Cl nuclei fixed at $r_2 = 6.2\ a_0$. x_H and y_H are the Cartesian coordinates of the proton relative to the Ar–Cl center of mass.

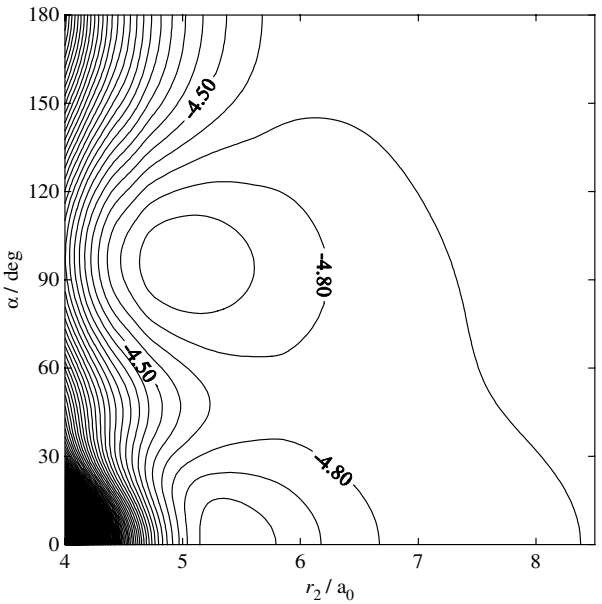

Fig. 4. DIM contour-line diagram of the potential-energy function $U(r_2, \alpha)$ for the electronic ground state of $ArHCl^+$. The H–Cl distance r_1 is fixed at 2.5 a_0.

[2] More information can be obtained on request from one of the authors by e-mail: ritschel@chem.uni-potsdam.de

Table 2. Molecular characteristics of $ArHCl^+$ in the lowest $^2A'$ state from recent conventional MO-based ab-initio studies and from the "minimal ab-initio DIM model".

	Geometry			Det. Energy[a]	Frequencies[b]			ZPE[c]	Atomic charges[d]		
	r_1	r_2	α	E_D	ω_1	ω_2	ω_3		q(Ar)	q(H)	q(Cl)
	a_0	a_0	deg	eV		cm^{-1}		eV		a.u.	
$ArHCl^+$ linear (Min1)											
Lundell et al. [3]											
MP2	2.58	6.17	0	−0.37	162	411/477	2153	0.199	0.139	0.485	0.376
CCSD(T)	2.58	6.18	0	–	–	–	–	–	–	–	–
Li et al. [4]											
MP2	2.50	6.53	0	−0.17	113	386/408	2556	0.215	0.073	0.252	0.675
QCISD	2.49	6.62	0	−0.16	109	356/380	2592	0.213	0.075	0.233	0.691
Neumann et al. [5][e]											
MRDCI	2.55	6.60	0	−0.15	119	390	2322	0.200	0.017	0.253	0.730
Present work											
CCSD	2.55	6.28	0	−0.27	150	395	2257	0.198	0.066	0.404	0.530
MRCI	2.56	6.26	0	−0.27	149	384	2204	0.194	0.075	0.394	0.531
DIM	2.62	5.44	0	−0.47	309	488	2672	0.245	0.192	0.474	0.334
$ArHCl^+$ bent (Min2)											
Lundell et al. [3]											
MP2	2.47	5.23	82.5	−0.22	148	336	2794	0.203	0.123	0.539	0.338
CCSD(T)	2.48	5.24	80.9	–	–	–	–	–	–	–	–
Li et al. [4]	–	–	–	–	–	–	–	–	–	–	–
Neumann et al. [5][e]											
MRDCI	2.50	5.28	92.4	−0.14	125	361	2672	0.196	0.161	0.238	0.601
Present work											
CCSD	2.47	5.05	87.3	−0.29	171	401	2766	0.207	0.101	0.352	0.547
MRCI	2.47	5.01	87.6	−0.30	184	429	2774	0.210	0.176	0.321	0.502
DIM	2.48	4.98	95.5	−0.33	190	569	2710	0.215	0.209	0.466	0.325
Saddle point bent (SP1)											
Present work											
CCSD	2.49	6.07	43.5	−0.17	134	268i	2688	0.175	0.028	0.368	0.603
MRCI	2.49	6.02	43.4	−0.16					0.032	0.330	0.638
DIM	2.50	5.87	49.0	−0.13	133	269i	2596	0.169	0.041	0.466	0.493
Saddle point $ArClH^+$ linear (SP2)											
Present work											
CCSD	2.49	6.21	180	−0.087	73	136i	2708	0.172	0.013	0.346	0.641
MRCI	2.49	6.17	180	−0.071					0.009	0.327	0.664
DIM	2.49	6.63	180	−0.032	58	103i	2760	0.175	0.001	0.469	0.530
Experiment											
Li et al. [4]	–	–	–	−0.27	–	–	–	–	–	–	–

[a] Argon-atom detachment energy E_D: total energy relative to the dissociation limit $Ar(^1S) + HCl^+(X^2\Pi)$. [b] Harmonic approximation. The numbering is: 1 – Ar–HCl stretch, 2 – ArHCl(Min1)/ArClH(Min2) bend, 3 – H–Cl stretch. [c] Zero-point vibrational energy calculated from the harmonic frequencies. [d] For the MO-based conventional methods, the atomic charges are obtained from Mulliken gross atomic populations (since CCSD charges cannot be calculated with MOLPRO, CISD data for CCSD geometries are given instead). In the DIM treatment, the atomic charges are deduced from the coefficients of the valence-bond-type structures, neglecting their overlap. Therefore the two sets of atomic charges can only be compared qualitatively. [e] Improved calculations, therefore slight differences from [5].

be verified by using the frequency data in Tables 1 and 2. For completeness we note that there is a third local minimum corresponding to a linear complex $(H–Ar–Cl)^+$ with $r_1 = 8.47\ a_0$, $r_2 = 6.04\ a_0$, and $\alpha = 0°$, i.e. H on the Ar side, lying 1.28 eV above the $Ar(^1S) + HCl^+(X^2\Pi)$ dissociation limit. Fragmentation of this complex is hindered by a flat barrier (some 0.1 eV); it plays no role in the low-energy dynamics or in determining the structure. This is entirely in accordance with our earlier findings [5].

2. The two relevant local minima on the ground-state PES are separated by a comparatively low barrier $\Delta U^{\ddagger}(SP1) = E_D(SP1) - E_D(Min1)$ (around 0.1 eV height if calculated by CCSD and MRCI as in the present treatment, see Tab. 2), so that the complex is expected to be somewhat floppy (see also [5]).
3. From a comparison with the experimental information about E_D [4] (see bottom line of Tab. 2), one cannot draw any definite conclusion concerning a possible preference for one or the other of the two geometric

structures of the complex, the more so as the barriers between the two minima are not very high. All the MO-based conventional ab-initio treatments lie within ±0.1 eV of the experimental E_D-value of Li et al. [4].

4. The molecular data obtained in the present work from conventional ab-initio approaches (CCSD, MRCI) are supported by the earlier studies and are consistent with the following qualitative conception of bonding in $ArHCl^+$ (see also [5]):
   (i) Taking a crude picture, the complex is held together by covalent (overlap-determined) and by electrostatic polarization (inductive) forces.
   It should be noted that this is an interpretational model only. It does not mean, in particular, inclusion of 3-body inductive terms in the DIM ansatz (see, e.g. [14]); our DIM model is still "minimal".
   (ii) In the linear structure (corresponding to Min1 of the ground-state PES), we find the $(H–Cl)^+$ bond to be almost as strong as in the free HCl^+ molecular ion but the $(Ar–HCl)^+$ attraction is weak. An analysis of the MO properties and Mulliken populations shows that the latter attraction has a small component originating from overlap between partially depopulated (about $0.07e$ charge transfer $Ar \rightarrow HCl^+$) $3s$ and $3p$ AOs of Ar with corresponding MOs of HCl^+, and a much larger component due to induced polarization, which we determined by a rough estimate of the pairwise ion-induced dipole interaction.
   This situation is reflected in a somewhat elongated H–Cl internuclear distance r_1, a lowered H–Cl stretch frequency ω_3 compared with the free HCl^+ molecular ion (see Tab. 1), a relatively large $Ar–HCl^+$ inter-fragment distance, the rather small E_D value, and the low frequency ω_1.
   (iii) In the nearly rectangular bent structure (Min2), the overlap-induced bonding properties are similar to those in the linear structure, with the HCl^+ fragment even less influenced by the presence of the Ar atom. This can also be seen from the MO properties, the Mulliken population analysis, and the values r_1 and ω_3, which are very close to those in the free HCl^+ (see Tab. 1). Again, the binding of the Ar to HCl^+ is dominanted by polarization (inductive) forces; an estimate yields nearly the same contribution to the stabilization energy as in the linear structure (within ca. 10%). Thus the analysis makes it understandable that the inter-fragment binding strength, if measured by the value of E_D, is about the same for the two structures of the triatomic complex.

   NB: This consideration only holds for the advanced ab-initio treatments referred to in Table 2. The detailed interplay between covalent and electrostatic interactions seems to be rather delicate, leading to the differences between the results of the various studies.
5. The DIM results (see Tab. 2) show an overall similarity to the data from the conventional MO-based ab-initio calculations but there are also several marked differences. A comparison reveals the following:
   (a) Our "minimal ab-initio DIM model" also shows two stable geometric structures for the $ArHCl^+$ complex: one exactly linear, $(Ar–H–Cl)^+$, and the other bent and nearly rectangular with an angle α somewhat too large.
   (b) In most of the MO-based conventional ab-initio work (except for the study by Lundell et al. [3]) the two structures have about the same stability but in our DIM treatment the linear complex (Min1) is distinctly more stable than the bent one (Min2). Furthermore, the barriers between the potential-energy minima are higher in the present DIM model.
   (c) The molecular characteristics for the two structures as calculated with DIM show some remarkable peculiarities. Important to note that the chances for analysing the wavefunctions and charge distributions are severely more restricted in the DIM approach than in conventional treatments working with explicit wavefunctions. In DIM we have access only to coefficients of VB structures in the wavefunction and to crude approximations of atomic charges (see footnote *d* to Tab. 2), and we may estimate polarization energy contributions using data from atomic/ionic polarizabilities (experimental or calculated with some approximate wavefunctions). Therefore all conclusions from such considerations have to be taken with due caution.
      – The first striking observation is that with DIM we obtain atomic charges clearly different from those in MO-based conventional ab-initio approaches as applied here. DIM yields more charge transfer $Ar \rightarrow HCl^+$, and the HCl^+ has the wrong polarity: the H end is more positive than the Cl end (q(H) is too large, q(Cl) too small). Presumably, this discrepancy is a consequence of the "minimal" DIM ansatz in combination with the mixing coefficients employed. This finding holds for both structures; the DIM atomic charges (like those in the conventional treatments, vide supra) do not differ very much for the two structures.
      – Owing to these deviations of the charge distribution and taking also into account an estimate of the attractive polarization (ion–induced dipole) interaction, we get with DIM a stronger stabilization compared with the conventional treatments, slight in the bent structure but marked in the linear structure.
      – These observations are clearly reflected in the molecular parameters (see Tab. 2):
      for the rectangular structure (Min2) of the complex, the DIM results are relatively close to those from the conventional ab-initio reference methods. This holds mainly for the distances r_1 and r_2, the Ar-detachment energy E_D, and the frequencies ω_1 and ω_3, whereas

Table 3. Electronic vertical spectrum of $ArHCl^+$ for excitation from the two ground-state structures corresponding to the local minima Min1 and Min2; DIM and MRCI results (present study) vs. MRDCI results [5]. Also shown are the respective asymptotic dissociation limits.

State	ΔU^* [a]			|TDME| [b]		Asymptotic limit	ΔU [c]
	DIM	MRCI	MRDCI	MRCI	MRDCI		
	eV	eV	eV	a.u.	a.u.		eV
(a) Min1 ($C_{\infty v}$)							
$X^2\Pi$	0.0	0.0	0.0			$Ar(^1S) + HCl^+(X^2\Pi)$	0.47
$1^2\Sigma^+$	2.82	2.63	2.83	0.102	0.099	$Ar^+(^2P^\circ) + HCl(X^1\Sigma^+)$	3.39
$2^2\Pi$	5.64	4.15	3.94	0.151	0.153		
$2^2\Sigma^+$	7.74	5.34	5.17	0.096	0.089	$Ar(^1S) + HCl^+(A^2\Sigma^+)$	4.04
(b) Min2 (C_s)							
X^2A'	0.0	0.0	0.0			$Ar(^1S) + HCl^+(X^2\Pi)$	0.33
$1^2A''$	0.87	0.79	0.58	0.013	0.020		
$2^2A'$	3.30	3.52	3.32	0.203	0.159	$Ar^+(^2P^\circ) + HCl(X^1\Sigma^+)$	3.25
$2^2A''$	3.35	3.65	3.38	0.053	0.025		
$3^2A'$	3.88	4.12	3.80	1.658	1.650		
$4^2A'$	4.93	4.85	4.67	0.295	0.026[d]	$Ar(^1S) + HCl^+(A^2\Sigma^+)$	3.90

[a] Vertical excitation energy ΔU^* relative to the respective PES local minimum (Min1 and Min2). [b] Transition-dipole matrix element, for MRCI and MRDCI only (see footnote 3 to the text). [c] ΔU is the total energy of the fragments measured relative to the energy of the ground-state potential minimum (Min1 and Min2, respectively). [d] This value, obtained in the earlier study, is probably in error.

the bending angle α and frequency ω_2 deviate more from the other treatments as expected for flat parts of the PES;
for the linear structure (Min1), the inter-fragment distance R (i.e. the distance of the Ar nucleus from the center of mass of HCl, not much different from r_2) is much too short in the DIM approach and the absolute value of the Ar-atom detachment energy E_D as well as the frequency ω_1 are too large. Moreover, the bending frequency ω_2 is higher with DIM.

– The saddle-point geometries are astonishingly well described by DIM as are the frequencies and the small magnitude of the inter-fragment charge transfer. In contrast, the DIM energies are in general rather more sensitive to changes in geometry than in the conventional ab-initio treatments.

Altogether we may draw the tentative conclusion that, despite some shortcomings in detail, our "minimal ab-initio DIM model" describes the complex $ArHCl^+$ to a crude but qualitatively acceptable approximation. The findings engender confidence in our extension of such DIM treatment to larger clusters Ar_nHCl^+.

4.1.2 Low-lying excited electronic states of $ArHCl^+$

The DIM approach is able to generate not only the PES for the electronic ground state but also, without any additional expense, the PES for each excited electronic state implied by the DIM basis. In order to get an overview of the electronic spectral properties and possible photo-processes, the relevant data characterizing the electronic vertical spectrum, namely the energy spacings ΔU and the transition-dipole matrix elements (TDME) between the ground state and excited states lying up to about 8 eV over the ground state are provided by Table 3 for each of the two relevant local-minimum structures of the ground-state $ArHCl^+$ complex[3].

First of all, there is good agreement between the two ab-initio multi-reference-CI sets of data to within a few 0.1 eV as can be expected for an AO basis set not particularly designed for excited-state calculations. The DIM results are in accordance with these data on the whole, much more so for the bent structure (Min2) than for the linear structure (Min1). This is another instance of the somewhat worse description of the complex in the linear configuration.

From the transition-dipole matrix elements it can be inferred that, in the energy range up to about 8 eV, electronic transitions can be expected to occur with highest probability from the ground-state linear complex to the $2^2\Pi$ state and from the ground-state bent complex to the states $3^2A'$ (correlating with $2^2\Pi$) and $2^2A'$ (correlating with $1^1\Sigma^+$); hence, it is these states that should be relevant to spectroscopy and photo-processes.

The lowest excited electronic state having a significant TDME value for excitation from the ground state is the $2^2A'$ state. Therefore it will be considered here in somewhat more detail. For comparison see also the discussion in [5]. In Figure 5 a contour plot of the potential-energy function $U(r_2, \alpha)$ as calculated with the present DIM model is shown and in Table 4 the molecular characteristics for the relevant stationary points of the $2^2A'$ PES are compiled for both the DIM and several conventional MO-based treatments. This is probably the first quantitative comparison of a DIM-generated *excited*-state PES

[3] The TDME values are obtained from the MRCI resp. MRDCI approach since DIM does not operate with explicit wavefunctions.

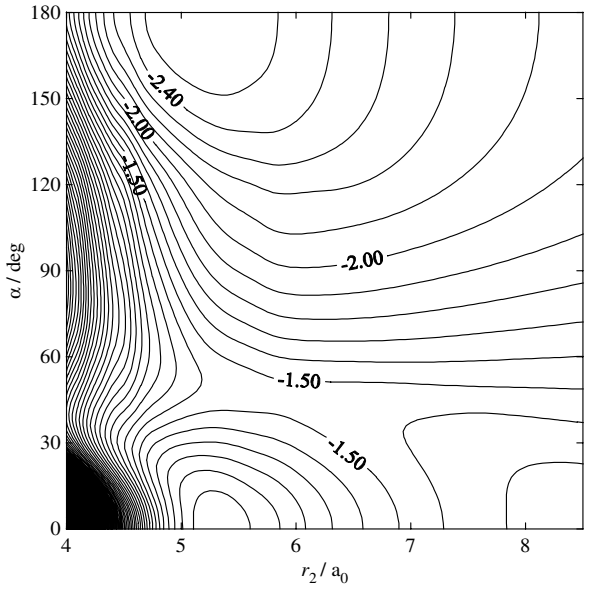

Fig. 5. DIM contour-line diagram of $U(r_2, \alpha)$ for the $2^2A'$ excited state of $ArHCl^+$. The H–Cl distance r_1 is fixed at 2.5 a_0.

with corresponding PESs from advanced MO-based conventional ab-initio procedures.

The energetics and topography of the $2^2A'$ PES obtained in an ab-initio MRDCI treatment have been discussed in detail in an earlier paper [5]. Taking this together with the results of the present study, we summarize here the main findings (see Fig. 5 and Tab. 4):

(i) Letting $r_2 \rightarrow \infty$, the $2^2A'$ state of $ArHCl^+$ correlates with the separated fragments $Ar^+(^2P^\circ)$ + $HCl(X^1\Sigma^+)$, which differ by a charge transfer from the corresponding ground-state fragments. Letting $r_1 \rightarrow \infty$, it correlates with $ArH^+(X^1\Sigma^+)$ + $Cl(^2P^\circ)$. Between these two asymptotic regions there is a large area of high potential-energy values and a saddle point (SP1′). On the Ar^+–HCl side, the PES exhibits a marked minimum (Min1′) for a linear atomic arrangement $(Ar–Cl–H)^+$; its depth is obtained in all available calculations to be about 0.9 eV relative to the $Ar^+(^2P^\circ)$ + $HCl(X^1\Sigma^+)$ dissociation limit (see Tab. 4). On the ArH^+–Cl side there is no significant minimum.

(ii) Taking the results of the advanced-level conventional ab-initio treatments as a guide, we observe marked differences in the molecular characteristics of the electronically excited complex (see Tab. 4), compared to the ground state (see Tab. 2). As in our considerations for the ground state, we find that the charge shift from the $HCl(X^1\Sigma^+)$ to the $Ar^+(^2P^\circ)$ ion is much larger (namely $0.36e$) than in both of the ground-state structures. Supported also by an analysis of the wavefunction (Mulliken overlap populations, binding-MO properties), we conclude that we have here a covalent-ionic (overlap-induced) bond Ar^+–ClH, which is stronger than in the linear ground-state structure $Ar–HCl^+$; concomitantly the H–Cl bond is somewhat weakened in comparison with the free HCl ground-state molecule (bond distance r_1 enlarged, frequency ω_3 decreased). The polarization interaction can be estimated to be much smaller than in the ground state, mainly because of the very small Cl atomic charge (see Tab. 4). On balance there is a markedly larger fragmentation energy $E_D = 0.9$ eV (vs. 0.3 eV for the linear ground-state structure).

(iii) The minimal DIM model exaggerates the polarity of HCl, both for the free (neutral) $HCl(X^1\Sigma^+)$ molecule and even more so for the HCl fragment in the excited state of the complex considered here. Addition of the Ar^+ ion leads to a small shift of electronic charge from H to Cl (leaving, however, the HCl to a large extend intact, as comparison of the bond length r_1 and the frequency ω_3 with their values in the free molecule shows) and also to a little electronic charge transfer from HCl to Ar^+ (about $0.1e$), much less than in the CCSD/CISD or MRCI ab-initio treatments. Correspondingly, the covalent-ionic part of the Ar^+–ClH binding should be weak with DIM but, mainly because of the larger atomic charges, the polarization attraction is stronger, similar to that in the ground-state linear structure, so that in the balance the Ar^+–ClH bond is only slightly looser (somewhat lower Ar^+-ion detachment energy E_D and frequency ω_1, and longer distance r_2) than with conventional ab-initio methods. Altogether, there is a remarkable agreement in structure and energetics for the excited-state minimum (Min1′) as well as for the saddle point (SP1′) of the DIM model with the advanced conventional approaches.

We feel therefore justified to conclude that the present minimal ab-initio DIM model leads to an excited-state PES which is at least qualitatively realistic.

From the topography of the $1^2A'$ ground-state and the $2^2A'$ excited-state PESs, one can deduce a number of possible photo-processes that could follow an electronic excitation $1^2A' \rightarrow 2^2A'$. A detailed discussion based on our earlier MRDCI study is given in paper [5] and is qualitatively applicable to the present DIM results as well.

4.2 Structure and stability of small Ar_nHCl^+ clusters ($n > 1$)

The extension of the investigation to aggregates Ar_nHCl^+ with more than one Ar atom is, in principle, easily done. Including the few additional fragment states not appearing in the triatomic $ArHCl^+$ case (namely, the Ar_2, Ar_2^+, and $ArCl^-$ states) leads to a $(21n+12)$-dimensional DIM matrix that must be diagonalized. Compared with the conventional ab-initio techniques, the computational expense for DIM is much smaller but it is much higher compared with the simpler Ar_nH^+ case. Therefore, we restrict our study to relatively small systems, up to $n = 13$. This suffices to gain an insight into the building up of larger clusters. The investigations described in this part of our study are focused mainly on the electronic ground state of the clusters.

Table 4. Properties of the $2^2A'$ excited electronic state of $ArHCl^+$: characteristics of stationary points from conventional ab-initio studies and from the "minimal ab-initio DIM model".

	Geometry			Det. Energy[a]	Frequencies[b]			ZPE[c]	Atomic charges[d]		
	r_1	r_2	α	E'_D	ω_1	ω_2	ω_3		q(Ar)	q(H)	q(Cl)
	a_0	a_0	deg	eV		cm^{-1}		eV		a.u.	
$ArClH^+$ linear (Min1′)											
Neumann et al. [5][e]											
MRDCI	2.57	4.58	180	−0.88	320	838	2179	0.259			
Present work											
CCSD[f]	2.54	4.48	180	−0.91	304	1173	2310	0.307	0.638	0.323	0.039
MRCI	2.53	4.49	180	−0.97	299	1047	2367	0.295	0.570	0.337	0.093
DIM	2.44	5.16	180	−0.87	170	339	2815	0.227	0.908	0.589	−0.497
$ArHCl^+$ bent (SP1′)											
Neumann et al. [5][e]											
MRDCI	2.50	6.07	55.1	0.08	172	891i	1644	0.113			
Present work											
MRCI	2.46	6.11	55.5	0.04	95	893i	2424	0.156	0.813	0.240	−0.053
DIM	2.41	8.45	51.4	0.17	88	505i	3034	0.194	1.000	0.426	−0.426

[a] Argon-ion detachment energy E'_D: total energy, relative to the dissociation limit $Ar^+(^2P^\circ)$ + $HCl(X^1\Sigma^+)$. [b–e] See footnotes *b–e* to Table 2. [f] The CCSD program operates with fictitious C_{2v} symmetry, in which the electronic ground state $1^2A'$ (component of $X^2\Pi$), correlating with 1^2B_1, and the excited state $2^2A'$ ($1^2\Sigma^+$), correlating with 1^2A_1, belong to different irreducible representations and can therefore be calculated separately.

Table 5. Ground-state molecular characteristics of the most stable Ar_nHCl^+ cluster structures[a] for n = 1–3; upper line: CCSD results, lower line: DIM results. For completeness, each of the two relevant structures of the triatomic complex (n = 1) is included.

n[b]	E_D[c]	ZPE[d]	r_1[e]	r_2[e]	r_3[e]	α[e]	β[e]	q(H)[f]	q(Cl)[f]	q(Ar)[f]	q(Ar′)[f]
	eV	eV	a_0	a_0	a_0	deg	deg	a.u.	a.u.	a.u.	a.u.
1_1	−0.269	0.198	2.55	6.28	–	0	–	0.404	0.530	0.066	–
	−0.472	0.245	2.62	5.44	–	0	–	0.474	0.334	0.192	–
1_2	−0.292	0.207	2.47	–	5.05	–	87.3	0.352	0.547	–	0.101
	−0.330	0.215	2.48	–	4.98	–	95.5	0.466	0.325	–	0.209
2	−0.508	0.227	2.51	6.41	5.14	0	85.9	0.427	0.462	0.036	0.074
	−0.555	0.222	2.62	5.46	6.11	≈ 0	82.0	0.474	0.330	0.181	0.015
3	−0.667	0.236	2.50	6.45	5.40	0	83.1	0.457	0.445	0.025	0.037
	−0.639	0.228	2.61	5.49	6.11	0	81.8	0.474	0.328	0.172	0.013

[a] We denote the two distinct types of argon atoms by Ar and Ar′: Ar lies in line with the HCl^+ fragment, Ar′ outside. [b] For n = 1 the two relevant structures corresponding to Min1 and Min2 are distinguished by subscripts 1 and 2 respectively. [c] Argon detachment energy E_D: total energy relative to the dissociation limit $nAr(^1S)$ + $HCl^+(X^2\Pi)$. [d] See footnote *c* to Table 2. [e] r_1 is the H–Cl distance, r_2 and r_3 are the distances Ar–Cl and Ar′–Cl, respectively; α and β are the angles ∠ArClH and ∠Ar′ClH, respectively. [f] See footnote *d* to Table 2.

In order to make the building-up process somewhat more transparent, we follow the energetics of the clusters by means of the argon-atom detachment energy E_D, defined as the energy required for "peeling-off" all argon atoms from the cluster, as a function of the cluster size (n):

$$E_D(n) = E(Ar_nHCl^+) - nE(Ar) - E(HCl^+), \quad (1)$$

a generalization of the definition given in footnote *a* of Table 2; all species appearing are understood to be in their electronic ground states and the cluster is in its most stable structure corresponding to the global minimum of the PES. From this quantity, the binding energy of the last added Ar atom (no. n), the "Ar-atom vaporization energy", is obtained:

$$\begin{aligned} \Delta E(n) &= E(Ar_nHCl^+) - E(Ar_{n-1}HCl^+) \\ &= E_D(n) - E_D(n-1). \end{aligned} \quad (2)$$

To begin with, we underpin the DIM results by CCSD ab-initio calculations as far as it is feasible. Because of the higher electronic complexity, this part of the task must also be more restricted than for the simpler Ar_nH^+ case, namely up to n = 3 only.

We complete the section with a few remarks on the lowest excited states of Ar_nHCl^+ clusters.

4.2.1 Test of the DIM approach for small clusters

Table 5 compiles molecular characteristics for the most stable structures of clusters Ar_nHCl^+ with n = 1–3 in their electronic ground states as obtained from CCSD and DIM calculations. For the triatomic complex, information is given for each of the two relevant structures. The Ar-atom detachment energies for the species with n = 1–3

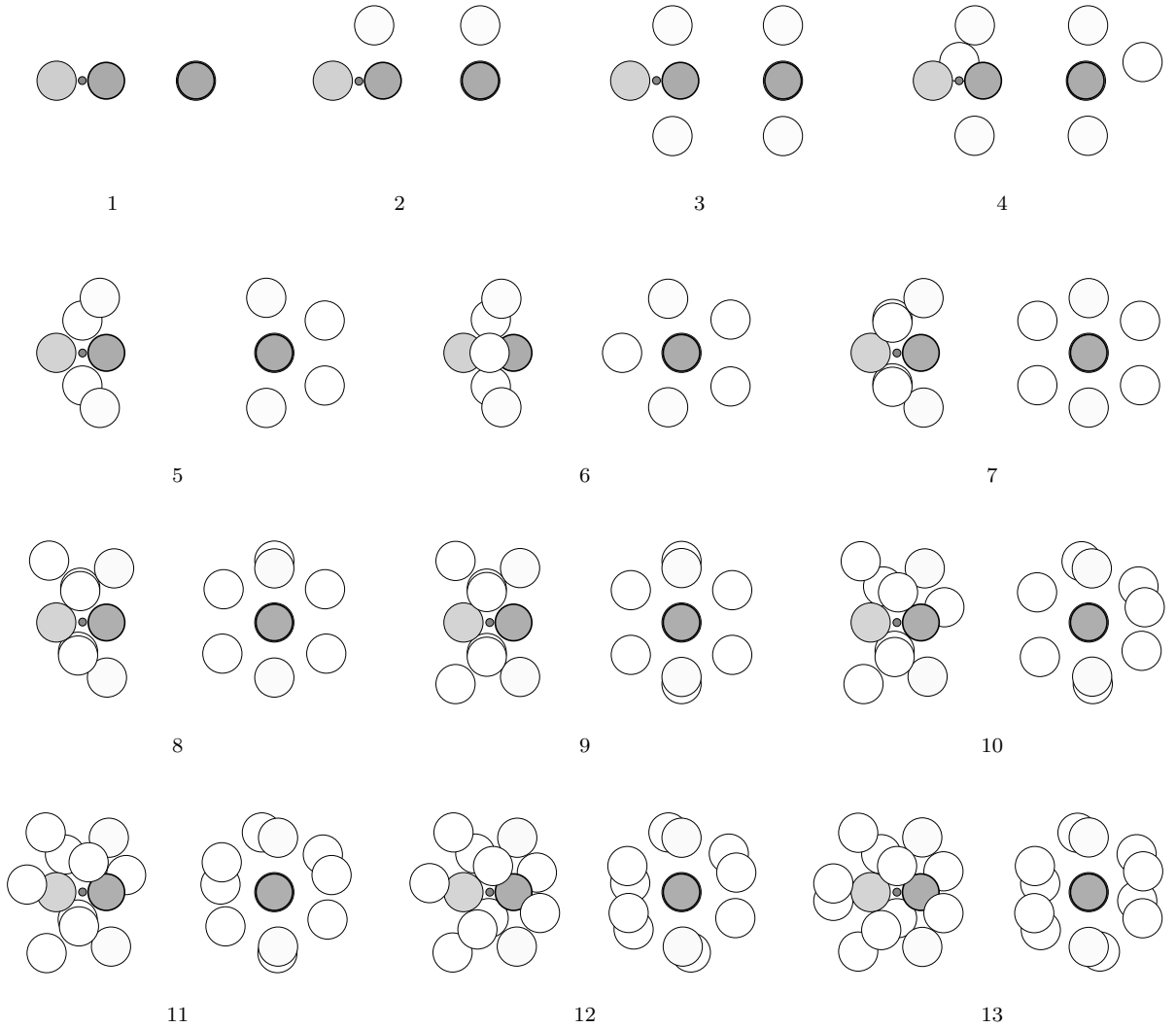

The atomic charge is indicated by the shading of the spheres: ● $q > 0.45\,e$, ● $0.3 < q < 0.35\,e$, ○ $0.15 < q < 0.2\,e$, ○ $q < 0.02\,e$.

Fig. 6. The most stable Ar_nHCl^+ cluster structures for $n = 1$–13 as obtained from the minimal DIM model. Each cluster is shown in side view facing the $(ArHCl)^+$ core (left part) and in end view along the $(ArHCl)^+$ axis (right part); the Cl-atom sphere in the core is marked by a heavier boundary line.

from the CCSD treatment are included in the left part of Figure 7a, and the structures obtained by DIM for each of the small clusters are seen in the upper left part of Figure 6.

The agreement of DIM with the CCSD results is of course not as good as in the case of the protonated argon clusters (see part I [1]). The discrepancy, however, is relatively small if we take for the triatomic complex ($n = 1$) the binding energy of the rectangular structure (Min2). This confirms our earlier observation (vide supra) that this bent structure is better described by DIM than the linear structure (Min1), for which the binding comes out too strong.

The discrepancy becomes less dramatic when more Ar atoms are added and the agreement of DIM with CCSD gets better for the E_D values as well as for the slope of the $E_D(n)$ line, whereby the binding seems to be systematically somewhat underestimated by DIM (as in the Ar_nH^+ case [1]): $|E_D^{DIM}| < |E_D^{CCSD}|$, ($E_D < 0$). As seen from the geometry data in Table 5, the CCSD approach adds the second Ar atom to an –H–Cl axial position on the H side of the bent $ArHCl^+$, whereas with DIM, in which the linear $ArHCl^+$ core is already the most stable arrangement, it is energetically most favourable to put the second Ar into a position in an equatorial plane. The result is an Ar_2HCl^+ structure of the same kind in both cases (the L-shape in Fig. 6). That one of the Ar atoms is positioned laterally in a plane containing the Ar–H–Cl axis and dragged markedly towards the Cl end of the axis is a result of the charge asymmetry and of the (weak) covalent binding from overlap between the outer π-type orbital of HCl^+ (in its $^2\Pi$ electronic ground state) and outer Ar orbitals, which may participate in binding because of partial depopulation by the electronic charge transfer from Ar to

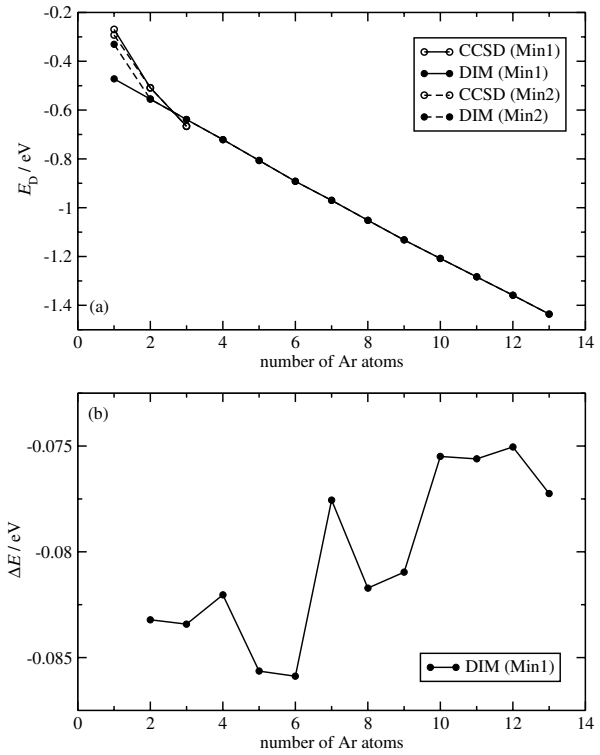

Fig. 7. DIM energy characteristics of Ar_nHCl^+ clusters (most stable structures in the electronic ground states) as functions of n: (a) Ar detachment energy, E_D, (i.e. the energy relative to the dissociation limit $n\mathrm{Ar}(^1\mathrm{S}) + \mathrm{HCl}^+(X^2\Pi)$), (b) binding energy of the last added Ar atom, ΔE.

HCl^+. The further building-up of the most stable cluster structures on adding more Ar atoms goes the same way in DIM and CCSD, the next cluster ($n = 3$) being a T-shape complex. The placement of the third Ar atom leading to this almost symmetrical planar arrangement is easily understood by an argument analogous to that for the $n = 2$ case.

The overall result is like that for the protonated argon clusters: a similar n-dependence of E_D (nearly linear) and ΔE in both the CCSD and DIM approaches, with an approximately parallel shift. This gives us confidence in the ability of DIM to predict the most stable structures of medium-sized Ar_nHCl^+ clusters.

4.2.2 Building-up of medium-sized clusters

The most stable DIM structures of the Ar_nHCl^+ clusters with $n = 1$–13 are depicted by the schematic diagrams in Figure 6. If we compare with the simpler Ar_nH^+ case (Fig. 6 in part I [1]), the main striking difference is the much less regular nature of the sequence of geometries here, pointing to the lack of a clear-cut building-up rule for positioning each newly added Ar atom. This is the consequence of the lack of symmetry of the core fragment $(Ar–H–Cl)^+$: first, we no longer have a "left-right" symmetry with respect to the proton in the middle (i.e. there is no inversion center) and secondly, there is no "rotational" symmetry about the core axis because the core electron hole is in a π orbital. Keeping this in mind, the stepwise building-up of the most stable cluster structures can be understood as follows.

The geometries of the complexes with $n = 2$ and 3 have already been interpreted in the foregoing section. The addition of further Ar atoms, one after the other, is determined essentially by the strength of the attractive electrostatic (polarization) forces, i.e. by the closest possible (by reason of steric repulsion) approaches to the differently positively charged constituents of the core fragment, and by the attractive dispersion-type interactions with the other extra-core Ar atoms. The last added Ar atom is usually placed as near to the core and to the other extra-core Ar atoms as the onset of steric repulsion allows.

Attention must be also paid to the Jahn-Teller effect, which prevents all these electronic open-shell aggregates from forming symmetrical structures.

In Figure 7 the two functions, $E_D(n)$ and $\Delta E(n)$, as obtained from the DIM calculations, are shown as graphs in the range of $n = 1$–13.

The relatively high stability of the clusters with $n = 2$ and 3, and the looser binding of the fourth Ar atom (for which only weak van-der-Waals attractions are acting) can be clearly recognized from the graph of Figure 7b. For $n = 5$, the "T-baulk" (having been formed by the two outer Ar atoms in Ar_3HCl^+) is somewhat pushed aside, thus enabling the other two Ar atoms (numbers 4 and 5) to come nearer to the charged core and leading to a significant gain in stability (i.e. energy decrease). The next Ar atom ($n = 6$) is attached to the other side of the T-shaped Ar_3HCl^+, and also for $n = 7$ the additional Ar atom is placed here, forming a four-membered ring that lies, roughly speaking, in an equatorial plane cutting the core axis close to the proton. In this latter structure the outer Ar atoms are arranged in a distorted six-membered ring ("boat-shape") which is a little expanded, and therefore the cluster is less stable.

Adding two more Ar atoms leads to completion of the structure by an Ar pair on the Ar side of the core, also relatively stable. With $n = 10$ a new, more loosely attached wrapper shell starts to build up, as reflected by a pronounced increase in the ΔE graph.

What is to be concluded from these considerations is that the structures of Ar_nHCl^+ clusters can be understood, to be sure, but the interpretation is by far not as simple and straightforward as in the case of the protonated argon clusters, Ar_nH^+ (see part I [1]). Therefore the cluster structure cannot be predicted without performing careful calculations, and the formulation of an additive increment scheme for the binding energy like that developed for the Ar_nH^+ case hardly seems feasible.

Up to this point, we considered only the *electronic* aspect of stability as it can be deduced directly from the PES data; all the structures shown in Figure 6 are "electronically stable" with respect to Ar-atom detachment, $Ar_nHCl^+ \rightarrow Ar + Ar_{n-1}HCl^+$ (the lowest-energy fragmentation channel). If we include the *zero-point vibration*, all these structures remain stable because the amount

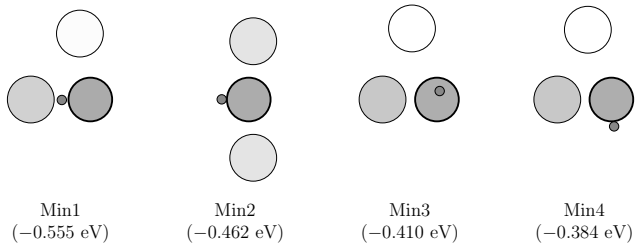

Fig. 8. The most stable and several less stable structures of the complex Ar_2HCl^+ (in parentheses: E_D).

of electronic stabilization energy $\Delta E(n)$ is always much larger (by an order of magnitude and more) than the concomitant destabilizing increase of the zero-point vibrational energy, $\Delta\mathrm{ZPE}(n) = \mathrm{ZPE}(n) - \mathrm{ZPE}(n-1)$. For $n = 1$–3 the ZPE data are given in Table 5. For the larger clusters, the magnitudes of the ZPE resp. ΔZPE remain in this energy range.

As discussed in some detail in Section 4.1.1, even for the simplest complex $ArHCl^+$ the ground-state PES possesses several minima: two marked minima corresponding to firmly stable structures with a comparatively low energy barrier between them plus a third, very weakly bound linear complex $Cl\cdots ArH^+$. We might therefore suppose the attachment of more Ar atoms to be accompanied by an increasingly broad variety of structures, some of them differing only slightly in energy and being separated by low barriers from each other. This is indeed the case; thus we expect the Ar_nHCl^+ clusters to show floppy behaviour. As an example, let us consider in Figure 8 several structures for the Ar_2HCl^+ complex, for which the geometrical forms are easily understood. The most stable structure (corresponding to the deepest minimum of the PES, Min1) represents a tightly bound, nearly linear $ArHCl^+$ core fragment with one extra lateral Ar atom, as discussed in the foregoing section. The next stable structure (Min2) can be considered as consisting of an HCl^+-like fragment with two Ar atoms laterally attached to it by weak covalent binding from the overlap of the lobes of the singly occupied π orbital of HCl^+ with Ar orbitals partly depopulated by charge transfer. The third and fourth electronically stable structures (Min3 and Min4) originate clearly from the bent $ArHCl^+$ form with one extra Ar atom added laterally to the $ArHCl^+$ triangle. At significantly higher energy there are a number of other structures held together by pure van-der-Waals attractions of one Ar and one Cl atom to the ArH^+ molecular ion, with no noticeable charge transfer. Such structures have no significance.

4.2.3 Low-lying excited electronic states of Ar_nHCl^+ ($n > 1$)

Just as for the protonated argon clusters (see part I [1], Sect. 3.3.2), it is interesting here also to inquire to what extent the low-energy part of the electronic term structure bears some relationship to that of the triatomic $ArHCl^+$ complex (vide supra). The situation, however, is more complicated in our case. Within the framework of the present paper, we cannot investigate this in full detail but we will give some information which should be sufficient for getting an overall first impression.

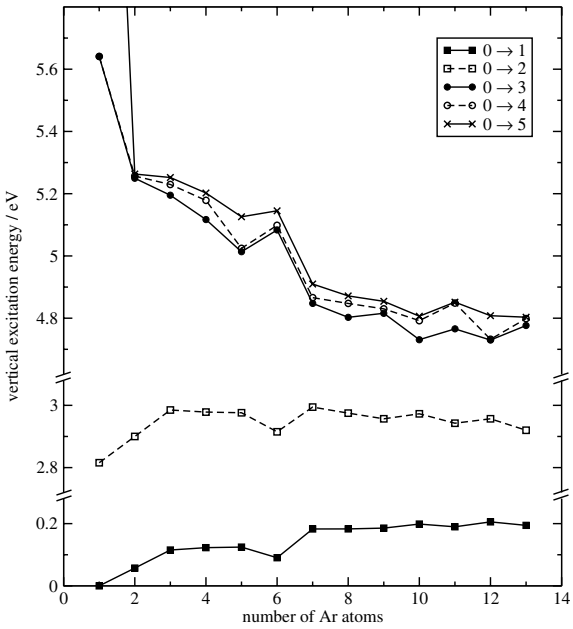

Fig. 9. DIM vertical excitation energies ΔU^* from the ground electronic state (i.e. the most stable structure for each cluster) of Ar_nHCl^+ clusters to the lowest five excited states as functions of n.

In Figure 9, the DIM transition energies ΔU^* for vertical excitation from the most stable electronic ground state of each cluster to the lowest five excited states are graphically represented as a function of the cluster size, $n = 1$–13. The numerical values are collected in Table 6. The lowest fragmentation limits, in which all Ar species (Ar or Ar^+) are stripped from the HCl^+ or HCl core fragment, can be inferred from Table 3. It should be noted, that the excited states are labelled only by numbers, since most of the clusters have no symmetry.

We first recognize from Figure 9, that there are indications of a certain bundling of the states in "bands", as is typical for all sorts of clusters. The spreading of the energy levels is largest for $n = 1$. With increasing n, a tendency for the excitation energies to approach nearly constant values is observed. This is easily understood, since Ar atoms tacked loosely to the $(Ar–H–Cl)^+$ ground-state core (see the discussion in the foregoing section) should not significantly affect the electronic spectrum. Thus the simple picture emerges that, as far as electronic excitation is concerned, it is only the $(Ar–H–Cl)^+$ core (common to all the most stable cluster structures in the electronic ground state, see Fig. 6) that plays a role, at least in the energy range considered.

In particular, the statement concerning the minor influence of the off-core Ar atoms should be true for the second excited state, i.e. the state no. 2 in the numbering of Table 6 and Figure 9. This state corresponds to the state $2^2A'$ (resp. $1^2\Sigma^+$) of the triatomic complex $ArHCl^+$, and therefore we expect for this second excited state of

Table 6. Electronic vertical spectra of Ar_nHCl^+ clusters with n = 1–13 Ar atoms, for transitions from the most stable ground-state structure in each case to the lowest five excited states (DIM results).

n	$\Delta U^*_{0\to1}$ eV	$\Delta U^*_{0\to2}$ eV	$\Delta U^*_{0\to3}$ eV	$\Delta U^*_{0\to4}$ eV	$\Delta U^*_{0\to5}$ eV
1	0.00	2.82	5.64	5.64	7.74
2	0.06	2.90	5.25	5.26	5.26
3	0.12	2.99	5.20	5.23	5.25
4	0.12	2.98	5.12	5.18	5.20
5	0.13	2.98	5.01	5.03	5.13
6	0.09	2.92	5.08	5.10	5.15
7	0.18	2.99	4.85	4.86	4.91
8	0.18	2.98	4.80	4.85	4.87
9	0.17	2.96	4.82	4.83	4.85
10	0.20	2.97	4.73	4.79	4.81
11	0.19	2.94	4.77	4.85	4.85
12	0.21	2.96	4.73	4.73	4.81
13	0.20	2.92	4.78	4.80	4.80

larger clusters a PES topography similar to that discussed for $2^2A'$ in Section 4.1.2, as far as the dependence on the core geometry parameters is concerned. However, it must be borne in mind that outer Ar atoms should hinder the HCl^+ (or HCl) fragment from turning from one equilibrium position into another one; i.e. the relevant barriers are expected to be enhanced on packing Ar atoms into the first wrapper cloud.

Some conclusions about the stability of the clusters following electronic excitation can be drawn from the data given (see Fig. 9). As we have seen in the foregoing section, the electronic ground state is stabilized with increasing cluster size (n) by around 0.08 eV for each attached Ar atom. The first excited electronic state ($1^2A''$ for the $ArHCl^+$ complex) lies rather close to the ground state. It is somewhat elevated when adding more Ar atoms but keeps a nearly constant excitation-energy value of about 0.2 eV for all the larger clusters with a linear $(Ar–H–Cl)^+$ core. For other geometries (see the value for the nearly rectangular structure of $ArHCl^+$, Min2, in Tab. 3: $\Delta U^* = 0.87$ eV), this state may lie energetically higher, and excitation to it from the ground state then leads to Ar atom detachment (for bent $ArHCl^+$ we have $\Delta U^*_{0\to1} > |E_D|$, the dissociation limit correlates with the state $1^2A''$ and with the ground state X^2A').

The second excited state for $n = 1$ is identical with our well-known $2^2A'$ state (see Sect. 4.1.2). If the complex is excited from the linear ground-state structure (Min1) to this state, we come up energetically below the fragmentation (Ar detachment) limit, i.e. the complex is stable for this excitation. For excitation from the bent ground-state structure (Min2) the excited complex has an energy close to the fragmentation limit and may be unstable. It should be pointed out again that, for a linear $(Ar–Cl–H)^+$ geometry, the excited-state PES has a pronounced minimum (see foregoing section and Tab. 4), which is just possibly accessible after the photo-excitation. A complete discussion of the stability of the second excited state of Ar_nHCl^+ clusters with $n > 1$ would require considering a relaxation of the geometrical configuration from the core structure Ar–H–Cl to Ar–Cl–H as well as a possible reorganization of the Ar wrapper as compared with that of the electronic ground state because of changes in the charge distribution. This would exceed the range of the present paper.

The third, fourth, and fifth vertically excited electronic states show a rather steep decrease as n increases from 1 to 7; on adding more Ar atoms, the $\Delta U^*_{0\to3\ldots5}$ graphs approach roughly constant values around 4.8 eV. Taking into account the stabilization of the electronic ground state with increasing n up to the cluster sizes considered, the clusters are unstable following vertical excitation into these electronic states: their energies lie above the respective fragmentation limits. However, it seems well possible that on attaching even more Ar atoms, these excited states will become stable after vertical excitation from the ground state for n somewhere between 15 and 20. Again, a more detailed discussion is not possible without investigating the PES topography and the relevant relaxation processes in these states.

5 Summary and conclusions

We have used our "minimal ab-initio DIM model" (with carefully prepared input data from accurate ab-initio computation of the atomic and diatomic fragments plus application of a wavefunction projection procedure) to extend the study of inhomogeneous cationic van-der-Waals clusters to argon clusters with an electronically complicated cationic impurity, the HCl^+ molecular ion, instead of a proton as in the first two papers of this series, which described the structure and the dynamics of Ar_nH^+ clusters quite satisfactorily. Because of the higher complexity of the electronic structure, the investigation was much more demanding and had to be restricted to clusters of up to 13 Ar atoms only.

The present paper reports on the results for binding and structure properties of these Ar_nHCl^+ clusters; the peculiar aspects of the study and the main findings are the following:

1. Compared with the investigation of Ar_nH^+ clusters, the "minimal DIM basis" for Ar_nHCl^+ had to include 18 atomic and diatomic fragments with altogether 57 electronic states (for Ar_nH^+ there were only 7 fragments and 12 states). Furthermore, a larger number of state manifolds contained several states of the same symmetry, which meant that mixing coefficients for up to four states were needed for the VB representation of the diatomic fragments (for Ar_nH^+ there was only one mixing of two states). Thus the computational effort was much greater but was still significantly below the expense for conventional ab-initio treatments.
2. For the smaller clusters, n = 1–3, ab-initio coupled-cluster (CCSD) cross-checking calculations were also carried out. Comparison with DIM shows larger deviations than in the Ar_nH^+ case, in particular for the triatomic complex ($n = 1$). The origin of these can be traced to an overestimation of the binding in the

linear $ArHCl^+$ complex by our DIM model. For the somewhat larger complexes the agreement gets better owing to a changing building-up mechanism and is estimated to result in a simple energetic shift. Because of the reasonable qualitative agreement, we are confident that our "minimal ab-initio DIM model" is a sufficiently reliable tool for describing even such complicated systems as Ar_nHCl^+ clusters at least qualitatively correctly.

3. The structures of Ar_nHCl^+ clusters at the global minima (the most stable structures) in the size range $n =$ 1–13 show some special features and are not as simple and easy to understand as for the Ar_nH^+ clusters. Similar to that case, the linear triatomic $ArHCl^+$ complex forms a core which remains essentially unchanged with increasing cluster size apart from some slight deformations. However, the building-up process is much less regular. This is recognized as originating from the lack of symmetry of the core fragment: there is no inversion center of the nuclear skeleton and no axial rotational symmetry of the electron cloud (which is in a Π state).
4. For each of the Ar_nHCl^+ aggregates, there are a variety of secondary less stable structures, some of them not much different in energy and separated by low barriers, so that the clusters should exhibit substantial floppy behaviour.
5. The energies of the low-lying excited electronic states are easily obtained within the framework of the DIM approach without additional effort and reflect a rather complex electronic structure resulting in a richer topography of the corresponding PESs. We studied the first $^2A'$ excited state (namely $2^2A'$) of $ArHCl^+$ in some detail. Further aspects of the excited electronic states of the larger medium-sized clusters were also considered; in particular, the vertical electronic excitation energies to the lowest five excited states were estimated for $n =$ 1–13, and the stability of the clusters following vertical electronic excitation was discussed. It is expected that photo-induced processes and the spectroscopy of Ar_nHCl^+ clusters are rather complicated. To make definite predictions will require more extended separate studies.

We conclude that our "minimal ab-initio DIM model" has passed another test, demonstrating its predictive power and recommending itself for further investigations, not only into binding and structure properties, but also into the dynamics of this kind of polyatomic system.

References

1. T. Ritschel, P.J. Kuntz, L. Zülicke, Eur. Phys. J. D **33**, 421 (2005)
2. T. Ritschel, Ch. Zuhrt, L. Zülicke, P.J. Kuntz, Eur. Phys. J. D **41**, 127 (2007)
3. L. Lundell, M. Räsänen, H. Kunttu, J. Mol. Struct. (Theochem) **358**, 159 (1995)
4. Y. Li, X.-Y. Wang, X.-G. Zhang, L.-B. Li, N.-Q. Lu, L.-S. Sheng, Y.-W. Zhang, Chem. Phys. Lett. **278**, 63 (1997)
5. L. Zülicke, R. Neumann, Ch. Zuhrt, J. Schretter, Int. J. Quantum Chem. **80**, 486 (2000)
6. MOLPRO is a package of ab-initio programs written by H.-J. Werner, P.J. Knowles, with contributions from R.D. Amos, A. Bernhardsson, A. Berning, P. Celani, D.L. Cooper, M.J.O. Deegan, A.J. Dobbyn, F. Eckert, C. Hampel, G. Hetzer, T. Korona, R. Lindh, A.W. Lloyd, S.J. McNicholas, F.R. Manby, W. Meyer, M.E. Mura, A. Nicklass, P. Palmieri, R. Pitzer, G. Rauhut, M. Schütz, H. Stoll, A.J. Stone, R. Tarroni, T. Thorsteinsson
7. D.E. Woon, T.H. Dunning Jr, J. Chem. Phys. **99**, 3739 (1993); T.H. Dunning Jr, J. Chem. Phys. **90**, 1007 (1989)
8. P.J. Kuntz, J.L. Schreiber, J. Chem. Phys. **76**, 4120 (1982)
9. T. Ritschel, Diploma Thesis, University of Potsdam (1998)
10. K.P. Huber, G. Herzberg, *Molecular Spectra and Molecular Structure, IV. Constants of Diatomic Molecules* (Van Nostrand Reinhold, New York, 1979)
11. T. Lenzer, I. Yourshaw, M.R. Furlanetto, G. Reiser, D.M. Neumark, J. Chem. Phys. **110**, 9578 (1999)
12. S.F. Boys, F. Bernardi, Mol. Phys. **19**, 553 (1970)
13. P.J. Kuntz, R. Polák, Chem. Phys. **99**, 405 (1985)
14. N.L. Doltsinis, P.J. Knowles, F.Y. Naumkin, Mol. Phys. **96**, 749 (1999)